

THE MAGNETOSPHERE AND SOLAR WIND ENVIRONMENTS

MARC A. MURISON
Astronomical Applications Department, U.S. Naval Observatory, Washington, DC
murison@aa.usno.navy.mil

July 13, 1999

ABSTRACT

This note contains a brief review of solar wind and Earth magnetospheric environment properties.

Key words: solar wind — magnetosphere

1. INTRODUCTION

A question concerning FAME is whether or not passive means of applying correcting torques to the FAME spacecraft may be employed. Discontinuous methods such as hydrazine jets are objectionable for many reasons, which I will not address here (see e.g. Kovalevsky 1995, p. 207; Reasenberg and Phillips 1998). Two passive methods are solar radiation pressure and solar wind pressure. If radiation pressure torques are employed, and if the spacecraft is in a high enough orbit so that it loses the protection of the Earth's magnetosphere, one naturally wonders what might be the perturbative torques caused by the spacecraft plowing through the solar wind. In this Memo, I introduce, for reference, some basic background material on the Earth magnetosphere and solar wind environment. The effects of the solar wind on the spin dynamics of FAME are discussed elsewhere.

2. SOLAR WIND PROPERTIES

The solar wind consists mainly of protons and electrons with a few percent of α particles and other heavy nuclei. For practical considerations of pressure, then, we may treat the wind as an unsteady flow of protons.

At the flow origin ($R < 2-3 R_{\odot}$), the flow direction is nearly radial from the Sun. Near the Sun ($R < 10 R_{\odot}$), the plasma is embedded in the rotating field, and the field is strong enough to force corotation of the plasma. Hence the plasma particles are spun up and flung outward along the field lines, like beads on a wire. With increasing distance from the Sun, the field lines form a spiral pattern. Due to this *garden hose effect*, the interplanetary magnetic field (IMF) angle is about 43 degrees at the Earth. However, the solar wind velocity is still nearly radially outward from the Sun. Figure 1 is an illustrative sketch of the geometry. Aberration due to the Earth's orbital velocity will cause the solar wind to appear at an angle

$$\varphi \approx \frac{V_{orb}}{V_{wind}} \approx \frac{30 \text{ km/sec}}{400 \text{ km/sec}} \approx 4.3 \text{ deg} \quad (1)$$

with respect to the Sun direction.

There are usually 2-4 field sector boundary crossings per synodic rotation of the sun (27.5 days), and the Earth's orbital plane is inclined to the heliographic equator by 7.25 degrees.

The solar wind is "gusty" on timescales of minutes to hours. Typical solar wind velocities are 300-700 km/s. The velocity distribution peaks around 390 km/s, with a sharp drop-off at 300 km/s and an exponential tail longward of 400 km/s.

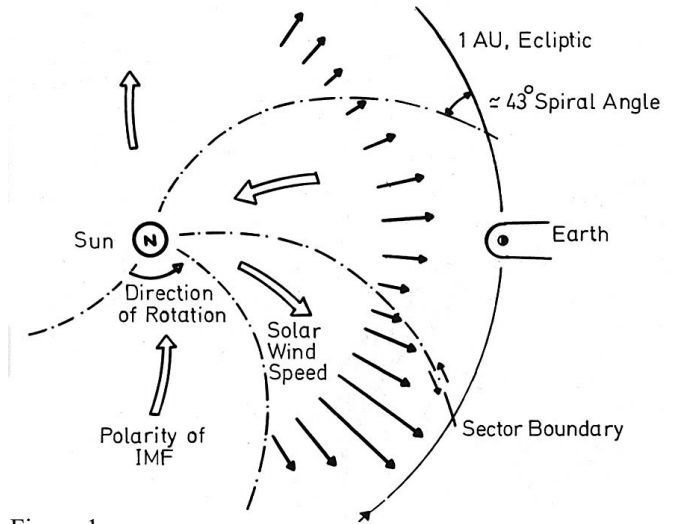


Figure 1

Figure 2 below shows the wind speed distribution for spacecraft data taken between 1962 and 1970. The solar wind particle density at 1 AU is in the range 2-20 cm^{-3} , typically 5-10 cm^{-3} . Proton energy is typically $\sim \frac{1}{2}$ -1 keV and electron energy is $\sim \frac{1}{4}$ keV.

Lang (1992) shows the following table, which is based on data from Feldman et al. (1977):

	mean	σ	median
N (cm^{-3})	8.7	6.6	6.9
V (km/s)	468	116	442

If the angle of incidence on a surface is χ , then, assuming pure absorption, the solar wind momentum transferred to a surface is

$$P_{\perp} = m_p N V^2 \cos^2 \chi \quad (2)$$

where m_p is the mass of the proton. For $\chi=0$, $N=10 \text{ cm}^{-3}$, $V=400 \text{ km s}^{-1}$, the pressure is about $P_{\perp} \sim 2.7 \times 10^{-9} \text{ Nm}^{-2}$, about a factor of a thousand smaller than that of the solar radiation pressure at 1 AU.

Figure 3 is a plot of SoHO proton data during January 1997.¹ (The SoHO spacecraft² is in a "halo" orbit about the Earth-Sun inner Lagrange point, roughly 200 Earth radii (R_E).

¹ Data from the SoHO CELIAS/MTOF Proton Monitor. See the web page <http://umtof.umd.edu/pm>

² For information about the SoHO mission, see the web page <http://sohowww.nascom.nasa.gov/>

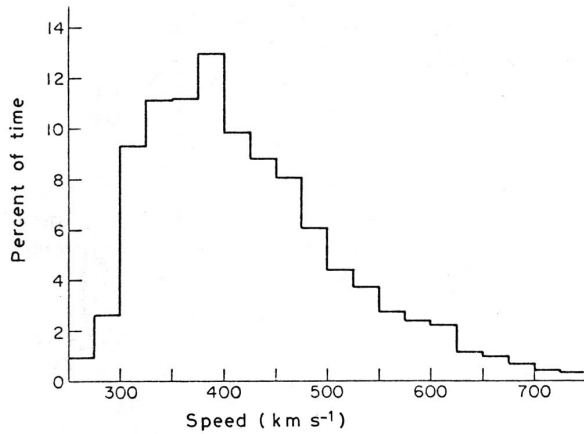


Figure 2

in the sunward direction.) The upper panel shows the solar wind speed in km/s, the center panel shows the proton number density in cm^{-3} (note the logarithmic scale), and the bottom panel plots the proton thermal speed in km/s. The large-amplitude fluctuation timescale is on the order of the solar rotation period. This corresponds to the large-scale features of the base of the solar corona, which is where the wind may be thought of as originating.

3. PROPERTIES OF THE EARTH'S MAGNETOSPHERE.

The magnetic field at the surface of the Earth is mainly that of a tilted, displaced dipole, but with fairly large distortions. The dipole offset from the Earth's center is roughly 450 km,

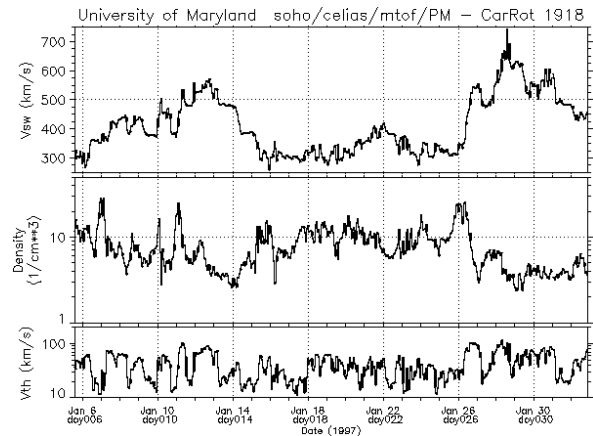


Figure 3

about 11.5 degrees. The mean field at the magnetic equator is 0.31 Gauss (G).³ Within a few radii of the Earth, the magnetic field approximates closely a potential field consisting of a dipole plus higher harmonics.

In the direction of the Sun, the geomagnetic field extends to about 10 R_E , a limit imposed by ram pressure from the solar wind (section 4). In the direction away from the Sun, the field is drawn out into a long magnetic tail. The detailed structure of the magnetosphere is quite complex and will not be discussed here. However, the cartoon in the following figure (Fig. 4) shows several of the main features.

The bow shock in the subsolar direction lives at about 15 R_E .

The magnetosheath (the region between magnetopause and bow shock) is 2-3 R_E thick at the subsolar point.

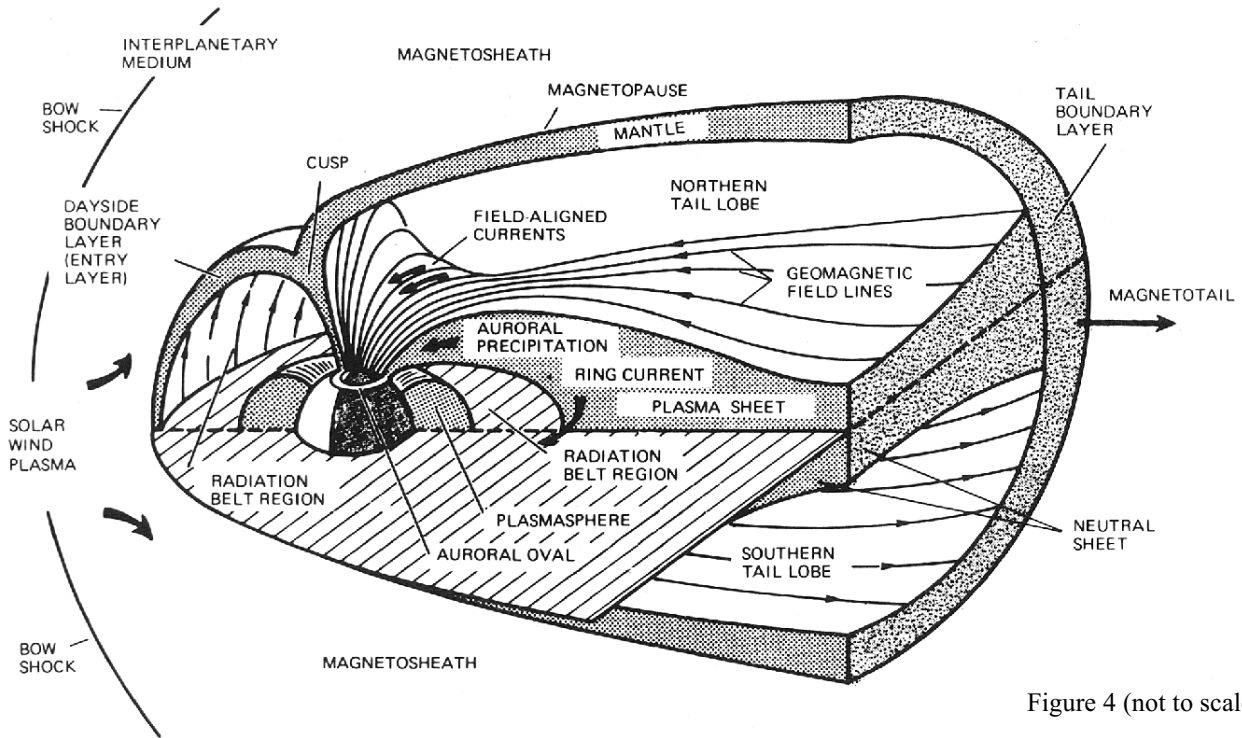


Figure 4 (not to scale!)

and the inclination of the dipole moment to the rotation axis is

³ The magnitudes of the second and third harmonics are one order of magnitude smaller: 0.043 G and 0.029 G.

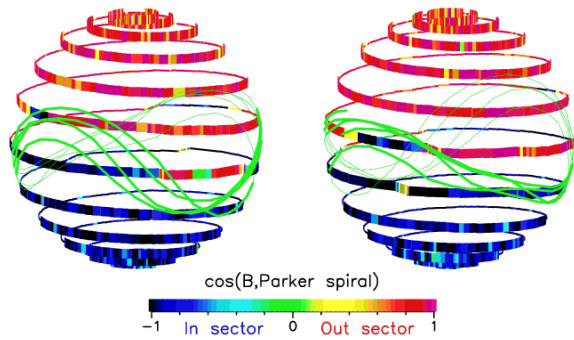


Figure 5. This plot shows the polarity of the magnetic field measured by the Ulysses spacecraft during the recent "fast latitude" scan, from 80°S to 80°N in around 12 months. The polarity is compared to the expected Parker spiral angle assuming an outward polarity field, allowing for changes in the solar wind speed, distance and latitude of the spacecraft. The colors correspond to the cosine of the angle between the Parker spiral direction and the measured field azimuth angle: red values indicate outward-pointing fields, while blue values show inward-pointing fields.

Figure 5 is an interesting color representation of the solar wind magnetic field polarity as recorded by the Ulysses spacecraft.⁴ Notice the skirt-like neutral sheet and the corresponding sector boundary crossings encountered in the equatorial plane.

4. APPROXIMATE LOCATION OF THE MAGNETOPAUSE SUBSOLAR POINT.

The magnetopause is the surface where the solar wind and geomagnetic field pressures balance. For wind particles of number density N , speed v , and mass m , impacting the surface at an angle ψ , the particle mass flux across the magnetopause is

$$\Phi_m = m N v \cos \psi \quad (3)$$

Assuming specular reflection at the magnetopause, the momentum change (i.e., the particle pressure) is then

$$P_{sw} = 2 m N v^2 \cos^2 \psi \quad (4)$$

Earth's magnetic field is roughly a dipole. Hence the field strength can be described by the scalar equation

The polarities are projected back to the "source surface" at a few solar radii, allowing for variable solar wind speeds. The rapid scan in latitude (due to the spacecraft's motion) and longitude (due to solar rotation) results in a "snapshot" of the heliospheric magnetic field at a period of low solar activity. The two views are simply opposite hemispheres of the same plot, from 60° and 240° central meridian longitude.

The inward polarity Southern polar regions and outward polarity Northern regions are clear in the plot, as is the asymmetric boundary between the two regions. The green lines indicate the calculated boundary at the "source surface" in the corona on the basis of measurements of the magnetic field in the photosphere, made at Wilcox Solar Observatory and published in the Solar Geophysical Data series. Each line corresponds to one solar rotation. Agreement between the calculations and observations is usually good, although there are some discrepancies: in particular, the boundary observed by Ulysses is generally at a lower latitude than that calculated for the corona, indicating that the boundary "flattens" with increasing distance from the Sun or that the model used to calculate the boundary in the corona overestimates the latitude range of the boundary.

$$B(r, \theta) \approx \frac{B_0}{r^3} \sqrt{1 + 3 \sin^2 \theta} \quad (5)$$

where r is in Earth radii, $B_0 = 0.306$ G is the geomagnetic field strength at the Earth's magnetic equator, and θ is the magnetic latitude.

The magnetic field pressure is $P_B = \frac{B^2}{8\pi}$. At the magnetopause the field lines are compressed due to the solar field being wrapped around the magnetopause, so as an approximation it is common to use roughly twice the value of the undisturbed geomagnetic field given by eq. (5). Equating P_B and P_{sw} , we find that the magnetopause distance in the subsolar direction ($\psi = \theta = 0$) is approximated by

$$r_0 = \left[\frac{B_0^2}{4 \pi m v^2 N} \right]^{\frac{1}{6}} \quad (6)$$

Using protons with $v = 400$ km/s and $N = 3 \text{ cm}^{-3}$, we obtain the subsolar point magnetopause at $R \approx 10 R_E$. The subsolar distance is usually in the range 9-11 R_E . During extremely disturbed conditions it may become as small as 6 R_E , exposing satellites in geosynchronous orbit.

REFERENCES AND BIBLIOGRAPHY

- Feldman, W.C., Asbridge, J.R., Bame, S.J., Gosling, J.T. (1977). "Plasma and Magnetic Fields from the Sun", in *The Solar Output and its Variations*, ed. O.R. White, Colorado Associated University Press, Boulder.
- Jackson, J.D. (1975). *Classical Electrodynamics*, 2nd edition, Wiley.
- Hargreaves, J.K. (1979). *The Upper Atmosphere and Solar-Terrestrial Relations*, Van Nostrand Reinhold.
- Kovalevsky, J. (1995). *Modern Astrometry*, Springer.
- Lang, K.R. (1992). *Astrophysical Data: Planets and Stars*, Springer-Verlag.
- Papagiannis, M.D. (1972). *Space Physics and Space Astronomy*, Gordon and Breach.
- Parker, E.N. (1958). "Dynamics of the Interplanetary Gas and Magnetic Fields", *Ap. J.* **128**, 664.
- Parker, E.N. (1979). *Cosmical Magnetic Fields*, Oxford University Press.

⁴ Plot and quoted text copied from the Ulysses magnetometer group web page at <http://www.sp.ph.ic.ac.uk/Ulysses/Plots/sphere.html>

Piddington, J.H. (1981). *Cosmic Electrodynamics*, 2nd edition, Krieger.

Reasenber, R.D., and Phillips, J.D. (1998). Proc. SPIE Vol. 3356.

Volland, Hans (1984). *Atmospheric Electrodynamics*, Springer-Verlag.